Determination of Subsurface Hardness Gradients in Plastically Graded Materials via Surface Indentation

Michael A. Klecka

Ghatu Subhash[1]

e-mail: subhash@ufl.edu

Nagaraj K. Arakere

Department of Mechanical and Aerospace Engineering, University of Florida, P.O. Box 116250, Gainesville, FL 32611-6250

Graded materials with high surface hardness and ductile cores are popularly used in high performance bearing applications to resist surface wear and fatigue damage. The gradient in hardness with depth is commonly determined using micro-indentation on the cross section of the material which contains the gradation in microstructure or composition. In the current study, a novel method is proposed to predict the hardness gradient profile using solely surface indentations at a range of loads. The method does not require the graded material to be sectioned, and has practical utility in the surface treatment industry. Two case hardened steels, M-50 NiL and Pyrowear® 675, and a through-hardened M50 steel, are used as model materials to illustrate the concepts. For a material with a decreasing gradient in hardness, higher indent loads result in a lower measured hardness due to the influence of the softer subsurface layers. A power-law model is presented which relates the measured surface indentation hardness under increasing load to the subsurface gradient in hardness. It is shown that the response of the material is not influenced greatly by the absolute surface hardness value, but instead sensitive to the sharpness of the gradient in subsurface hardness beneath the indented region. The proposed approach is not specific to case hardened steels and can be used to determine the subsurface hardness gradient for any plastically graded material (PGM). [DOI: 10.1115/1.4003859]

Keywords: plastically graded material (PGM), hardness gradient, case hardening, indentation

Introduction

Graded materials are increasingly used in high performance engineering applications [1–3], such as bearings and gears, where the gradient in material properties is tailored to reduce the likelihood of both wear and fatigue damage. This behavior is typically achieved by producing a material with a hardened surface and softer core. The gradient in material properties can be achieved through the use of surface coatings, heat treatment procedures, or a variation in grain size or composition. In such a configuration, a material with a graded construction typically performs better than one composed of only uniform hardness [1–3]. For example, in the case of hardened bearing steels used in high performance bearing raceways, the ductile subsurface can accommodate deformation and resist crack initiation/propagation, while the hard surface layers enhance rolling contact fatigue life and inhibit excessive wear.

A variety of studies in the past have investigated the behavior of graded materials [3–12]. The majority of these materials included a gradient in either elastic properties or both elastic and plastic properties simultaneously. Such behavior is typically accomplished through the introduction of a gradient in microstructure (e.g., grain size), composition, or both as a function of depth. In commercially available carburized steels, the elastic properties remain relatively constant but the plastic properties (i.e., yield strength, hardening coefficient, and strain hardening exponent) vary as a function of depth. Depending on the application, the depth of the carburization can be altered to produce the desired gradient in the material. Other heat treatment processes such as nitriding, boriding, induction hardening, etc. are also used to increase resistance to wear and improve component life [13]. These methods also result in graded materials with hard exteriors and soft cores. For case hardened materials, literature on hardness with depth of the graded layer is readily available [6]. This data is typically employed as a simple means to determine the penetration depth of a heat treatment procedure. Such data, however, is rarely used in selection of proper gradients for high-performance applications, nor does it predict how the subsurface hardness influences the deformation behavior.

Recently, Branch et al. [14] presented an inverse analysis to examine the constitutive response of plastically graded materials. This investigation utilized surface and subsurface indentation combined with finite element analysis in order to determine the hardening behavior (flow curves as a function of depth) of carburized tool steels using indentation induced deformation. Nayebi et al. [11,12] also analyzed heat-treated tool steels with a gradient in hardness (yield strength), utilizing instrumented indentation and finite element models in order to predict the hardness versus depth profile of a heat-treated steel. By utilizing a modified rule of mixtures, the instrumented indentation loading curves were related back to the cumulative hardness gradient influencing the indent. Furthermore, Stephens et al. [15] proposed a finite element model, which depicts the behavior of materials with gradients in yield strength and/or elastic modulus, and indicated that different gradients in material properties can be tailored to enhance the performance of a component.

Gu et al. [6] used inverse analysis to characterize materials with graded layers composed of yttria partially stabilized zirconia and metallic bond coat (NiCrAlY) deposited by plasma spraying. The experimental procedure utilized multiple spherical indenters with radius on the same order as the deposited layer thickness. After conducting indents of various depths/loads, a finite element model was developed to determine the properties of the graded

[1]Corresponding author.

Contributed by the Tribology Division of ASME for publication in the JOURNAL OF TRIBOLOGY. Manuscript received November 21, 2010; final manuscript received March 7, 2011; published online July 7, 2011. Assoc. Editor: Thierry Blanchet.

material. Similarly, Choi et al. [9] conducted an in depth analysis of plastically graded materials (PGMs) with linear gradients in yield strength and no variation in elastic modulus or strain hardening. This analysis was verified in a companion paper [10] detailing a specially synthesized nanostructured Ni-W alloy with a linear gradient in hardness (yield strength), achieved through a linear variation in the grain size.

The majority of these studies utilize instrumented indentation, finite element models, multiple indenter geometries, or a combination of these methods. Many rely on tailor made materials designed exclusively (e.g., plasma coating, deposition methods, etc.) for the analysis of gradients with specific material properties. In order to determine the variation in hardness with depth, it is typically necessary to section, polish, and indent the cross section of a graded material. While testing in this manner is perfectly suitable at the material developmental stage, this requirement becomes labor intensive and prohibitively expensive with increasing number of samples or at production levels. Alternatively, the current study aims to develop an approach for determining the nature of gradients beneath the surface, solely from surface hardness measurements. Such a method has practical utility in the surface heat-treatment industry, where the effectiveness of an intended heat-treatment process can be assessed by simple surface hardness measurements in order to determine the resulting gradient in mechanical property variation with depth. The result will also provide insight into the level of influence the deeper layers of a graded material may have on surface deformation, and how the gradient severity influences the surface hardness measurement.

Materials

Three commercially available bearing steels were employed as model materials in the current study: (i) a carburized stainless steel referred to as Pyroware® 675 (Carpenter Steel, Reading, PA), (ii) a carburized steel referred to as M-50 NiL, and (iii) a through-hardened M-50 steel [16–18]. The former two carburized materials, prior to carburization, contain only 0.1% carbon by weight. After carburization, the surface (case) layer can contain up to 1% carbon, with a gradient in carbon content that decreases as a function of depth. Heat treatment creates the final microstructure, consisting of tempered martensite and dispersed carbide particles of size less than 2 μm. The variation in carbon content and microstructure does not significantly alter the elastic properties, but results in a gradient in hardness (and yield strength) as a function of depth. The case layer of the carburized material exhibits extremely high hardness, with decreasing hardness over a depth of 2–3 mm (depending on material), until reaching the core material which has approximately half the surface hardness. This hardness gradient reflects a change in yield strength and work hardening behavior [14], and therefore the material behaves as a plastically graded material.

In order to first determine the hardness profile as a function of depth, specimens were ground and polished on surfaces parallel to the gradient direction (i.e., perpendicular to the hardest top surface). Polishing consisted of standard metallographic procedures, utilizing progressively smaller polishing media. Vickers microindents were produced on this surface at a load of 1 kg with a total loading duration of 15 s. These subsurface indents were spaced 100 μm apart to avoid interactions between neighboring indents, as per the ASTM standard E384 [19]. The resulting hardness profiles are plotted as a function of depth in Fig. 1. Differences in the hardness profiles are immediately noted when comparing these materials. The starting surface hardness of the P675 is more than 100 kg/mm^2 greater than that of the M-50 NiL material (920 kg/mm^2 for P675 versus 803 kg/mm^2 for M-50 NiL). While the P675 has a steep, decreasing gradient over the first 1.5 mm depth, the M-50 NiL has a gradually decreasing hardness profile over 2.5 mm depth. Additionally, the M-50 NiL hardness profile contains a region of nearly constant high-hardness near the top surface over a depth of 0.5 mm. This appears as a "plateau" in the hardness-depth profile. Also included with the P675 and M-50 NiL plots in Fig. 1 is the hardness profile from the through-hardened M-50 steel, which displays a constant hardness of 790 kg/mm^2 throughout the thickness and provides a baseline to which the graded materials will later be compared.

Surface Indentation Scheme

While the above method (i.e., sectioning, polishing, and indenting) reveals the gradient in hardness on the cross section of a specimen, the goal of this study is to analyze whether the subsurface gradients can be captured using only surface indentations. Such a method can facilitate the prediction of gradients produced during heat treatment without the need for cross-sectioning. As such, the testing scheme consists of a series of static indentation tests at increasing loads on the top surface of the graded material. In order to encompass a wide range of loads, indentations were performed using both a standard commercial table-top Vickers hardness tester (Wilson® Tukon™ 2100B, for loads ranging from 200 g to 50 kg) and a table-top universal testing machine load frame (MTS Alliance™ RT/30, for loads above 50 kg) with Vickers indenter tip mounted and driven in load control. The resulting indentations were measured using an optical microscope in order to calculate hardness. This provided a simple experimental setup, without requiring load-displacement plots common to instrumented indentation. It should be noted that even under high indentation loads, the resulting indent depth reached a maximum of 125 μm, while the depth of the entire graded region is greater than 2 mm. Therefore, only a portion of the subsurface graded material is affected by the surface indentation.

To expand the available graded materials for analysis, additional samples were extracted from various subsections of the graded materials by removing (grinding/polishing) a portion of the surface graded layer. This resulted in additional graded specimens with different starting surface hardness values and different starting hardness gradients with depth. The objective was to understand how these two factors (i.e., surface hardness and subsurface hardness gradient) influence the observed change in surface hardness values with increasing indentation load. Preparation of these sections of new graded materials from the as-supplied carburized specimens requires precise removal of prescribed amounts of material in order to arrive at regions with desired starting hardness and hardness gradient of interest. This process is similar to any final machining or grinding operation which may occur after a part is heat treated (i.e., in order to meet specified dimensional tolerances), thus removing a portion of the upper case layer. The open symbols in Fig. 1 indicate the locations of

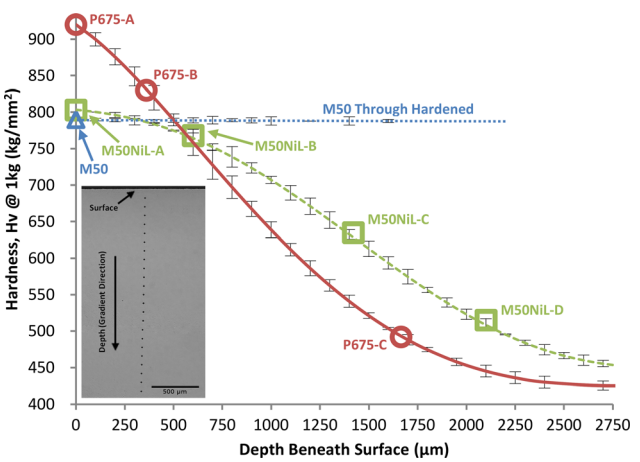

Fig. 1 Hardness profiles with depth for P675, M-50 NiL, and M-50 materials (trend-lines included for clarity). Unfilled symbols indicate locations of test sections. Inset micrograph reveals indents on the cross section of a specimen.

Table 1 Summary of material sections and relevant properties

Material/ section	Depth from original surface (μm)	Surface hardness Hv@1 kg (kg/mm^2)	Hardness gradient $\Delta Hv/\Delta x$ (Hv/mm)	Power-law "b" value
P675-A	0	920	−180	0.205
P675-B	350	822	−290	0.224
P675-C	1625	488	−155	0.175
M50NiL-A	0	803	−26	0.077
M50NiL-B	600	778	−112	0.166
M50NiL-C	1450	648	−196	0.207
M50NiL-D	2200	515	−130	0.181

the supplementary sections with different starting surface hardness and initial hardness gradients (i.e., local change in hardness at the surface as a function of depth, $\Delta H_v/\Delta x$) extracted for this study. Table 1 provides the relevant details along with the slopes of the hardness gradients for each location. Furthermore, because the P675 and M-50 NiL contain different initial gradients and surface hardness values, separating the effects of these two parameters required testing of sections with differing starting hardness yet comparable gradients (e.g., P675-A and M50NiL-C, see Table 1). This process aided in determining the sensitivity of the method to slight changes in initial hardness gradient and starting surface hardness. Finally, sections P675-C and M50NiL-D were selected due to their proximity to the transition between the graded layer and core material of constant hardness. The implications of this transition will be discussed in a later section.

Results

The variation in surface hardness values with increasing load on the as-received specimens with highest surface hardness are shown in Fig. 2 for both P675 and M-50 NiL materials (P675-A and M50NiL-A) in addition to the through-hardened M50. Both materials show higher hardness at low loads (200 g), revealing a slight indentation size effect (ISE). As the load P increases, the trend in hardness becomes more stable, reflecting the nature of the gradient beneath the surface. By conducting deeper (i.e., higher load) surface indents, the influence of the gradient in subsurface hardness can be inferred. As expected, there is an apparent reduction in hardness as the indentation load is increased. This behavior is anticipated, resulting from the influence of softer subsurface layers, which is more evident in the P675 specimen due to the sharper initial hardness gradient (see Fig. 1).

While the data in Fig. 2 is an indicator of how the material gradient influences the measured surface hardness under increasing indentation load, this data does not allow for direct comparison between sections with different starting surface hardness

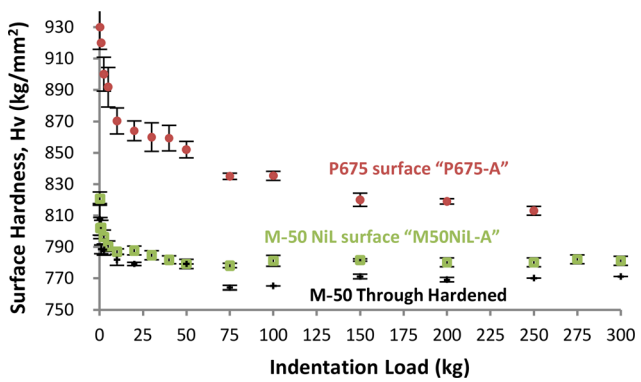

Fig. 2 Surface hardness versus load for M50 through-hardened and the hardest sections of both graded materials

values. In order to allow the data from many sections/materials with different surface hardness levels and gradients to be plotted simultaneously, a normalization scheme was adopted involving the surface hardness of each specimen tested. This normalization utilizes the surface hardness from each section (or subsection), measured at an indentation load of 1 kg. This load was chosen to minimize the influence of the subsurface gradients in measured hardness while reducing the influence of the indentation size effect. The indents produced at 1 kg have diagonal sizes of 30 μm or larger, while the grain size is an order of magnitude smaller [16,17].

In order to create dimensionless relationships for analysis, both indentation hardness and load were normalized based on the starting surface hardness and starting load (1 kg) for each section. The resulting plots of normalized hardness as a function of normalized indentation load are shown in Fig. 3 for the various subsections of the two materials, as well as for the through-hardened M50 steel which contains no hardness gradient with depth. Compared to Fig. 2 where the indentation size effect was prevalent at low loads, by plotting the curves with a staring load of 1 kg, the ISE has been significantly reduced. This is clearly evident in the plot of M50 through-hardened material which shows relatively a constant value of hardness with load. Although both P675 and M50-NiL appear to show indentation size effect (see Fig. 2), the decrease in hardness with increase in load is mostly due to the gradient in hardness with depth. The resulting data have been fit with power-law trend lines defined by $\bar{H} = -0.06\bar{P}^b + 1.06$, where $\bar{H}$ is the normalized hardness (i.e., hardness at that load over the hardness at 1 kg) and $\bar{P}$ is the normalized indentation load. These trends are used to illustrate the extent to which subsurface hardness gradients and starting surface hardness values influence the final observed surface hardness measurement under increasing indentation load. The power-law was chosen due to its simplicity and ability to fit the variety of graded sections.

Recalling the indicated starting slopes listed for the different subsections in Table 1 (i.e., starting gradient in hardness), a trend begins to emerge from the plots shown in Fig. 3. Materials with negligible gradients in hardness immediately beneath the surface (e.g., surface of M-50 NiL labeled M50NiL-A) show minimal change in hardness with increasing indentation load, nearly matching the behavior of the through-hardened M50 material which contains no gradient. However, as the severity of the subsurface hardness gradient increases (i.e., $\Delta H_v/\Delta x$), the reduction in surface hardness with increasing load becomes more prevalent. For instance, the M50NiL-B section with a mild gradient (−112 Hv/mm) shows a decrease in the surface indentation hardness of nearly 10% when load is increased from 1 to 300 kg, while the P675-B section with a severe gradient (−290 Hv/mm) decreases in hardness by 15% across the same load range. While this trend is expected, interestingly, it is also noted that the starting surface hardness value has little influence on the trends in normalized hardness versus load. This behavior is most evident when comparing data between specimens of similar gradient from two different materials with noticeably different starting surface hardness values. For example, the P675-A section has nearly the same hardness gradient as M50NiL-C (i.e., −180 versus −196 Hv/mm, respectively) but vastly different starting surface hardness values (920 kg/mm^2 for P675-A versus 648 kg/mm^2 for M50NiL-C). Nevertheless, they generate comparable trends in normalized surface hardness under increasing indentation load. This result indicates that the response of the plastically graded material is not influenced greatly by the absolute surface hardness value, but is instead sensitive to the sharpness of the gradient in subsurface hardness immediately beneath the indented region.

These trends in hardness as a function of increasing indentation load form the basis for an analytical method useful for determining unknown hardness gradients in a material by means of only surface indentation. In this method, the gradient in hardness as a function of depth is extracted from the curves shown in Fig. 1 and plotted, as shown in Fig. 4. The locations (depths) of the

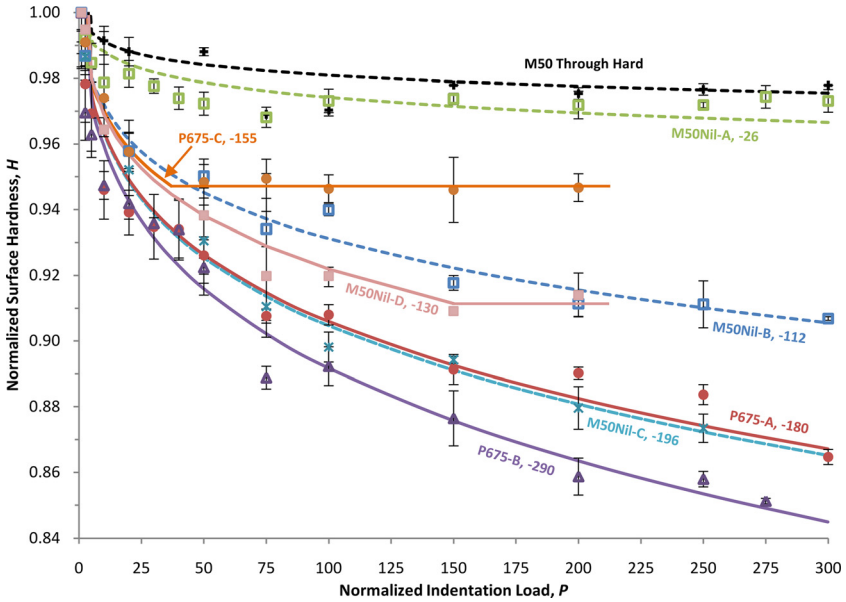

Fig. 3 Normalized surface hardness as a function of normalized indentation load for all sections and materials tested. The values shown next to each curve label indicates the initial hardness gradient for each section, i.e., change in hardness (kg/mm^2) over change in depth (mm) on the surface.

subsections are indicated by open symbols for each of the materials. Also included in this figure is a plot of the power-law exponents "b" (given in Table 1) from the corresponding test sections (from Fig. 3) as a function of hardness gradient. This plot of hardness gradient versus exponent values also follows a power-law curve fit, $\Delta H_v/\Delta x = 23500b^{3.0}$, providing a relationship between the hardness gradient and the behavior of the surface hardness under increasing indentation load. It can be seen from Fig. 4 and Table 1 that the higher the severity of hardness gradient, the higher the "b" value. Interestingly, irrespective of the material and starting surface hardness, all of the "b" values share a common curve.

Although further study is required in order to determine whether this relationship holds for a greater assortment of materials, the procedure described above can be applied to any graded material. Furthermore, any change in indenter geometry would affect measured hardness values [20] and trends and therefore may warrant a new analysis. For example, the deformation beneath a sharp indenter may extend deeper than that of a blunt indenter, thus the measured hardness will be influenced by the lower (softer) subsurface layers. This would alter the effect of subsurface gradients on measured hardness under increasing load.

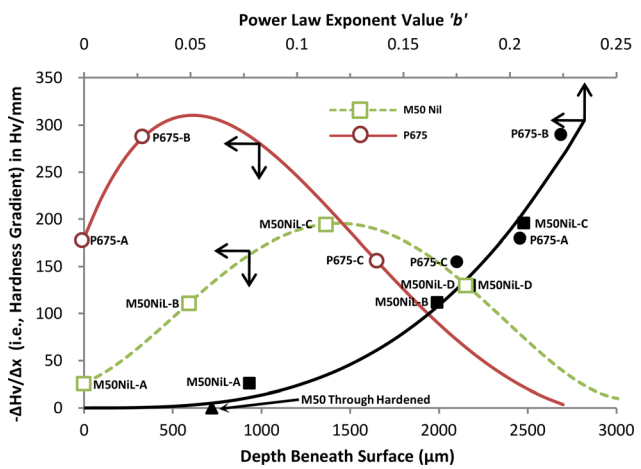

Fig. 4 Trend in hardness gradient and power-law exponent for both materials. Arrows indicate the axis to which the data refers to.

Detecting Changes in Gradient Trends. In addition to predicting the hardness profiles in graded materials, this technique has the ability to detect changes in the trends in subsurface hardness gradients. Such behavior occurs in regions where the graded layer transitions into the constant hardness core material. For example, consider the plots of P675-C and M50NiL-D (Fig. 3) which are near the core region. The trends in the data from these two sections initially appear similar to the data from other sections; however, there is a discontinuity at which the normalized hardness trends become constant. Interestingly, the point at which this behavior begins directly reflects the approximate location where the gradient in hardness ceases to exist and a constant core hardness begins.

It has been noted that the depth at which the plastic zone extends beneath a Vickers indentation is on the order of six to seven times the indent depth [21,22]. While this is applicable for homogenous materials, slight changes in the plastic zone have been shown for indentation on graded materials [14,15]. As such, this relationship will be utilized here only as a rule of thumb when noting the depth of indentation induced deformation. From the geometry of the Vickers indenter, the approximate indentation depth is related to the measured indent diagonal by a factor of 7 (i.e., the ratio of depth to diagonal length for the Vickers indenter geometry is 1/7). Thus, an approximate depth of the plastic zone can be predicted from the measured indent diagonal. While this does not take into consideration elastic recovery, it provides a reasonable estimate of the depth of an indentation and the associated deformation zone. For the two sections considered (P675-C and M50NiL-D), the transition to the core hardness level occurs at a depth of approximately 500–600 μm beneath the tested surface region (see Fig. 1). When the surface indents reach an approximate depth of one-seventh of this value (corresponding to the plastic zone depth of 500–600 μm), the trends in surface hardness with increasing load reach a constant value (i.e., flat regions of P675-C and M50NiL-D trends in Fig. 4). This sensitivity of the method to a changing hardness gradient provides an excellent means for detecting discontinuities in hardness gradient through the use of only surface indentation.

Conclusion

The results provided here indicate a practical relationship between the hardness measured via surface indentation under increasing loads and the severity of the subsurface gradient in hardness. It provides a rapid method for predicting the gradients produced during surface heat treatment, consisting of only a series of indentations at increasing loads on the sample surface, requiring only a hardness tester and minimal sample preparation. The results are then compared to the predetermined (calibrated) power-law trends in order to estimate the local hardness gradient. Here, larger exponent "*b*" values indicate more severe gradients, while "*b*" values approaching zero signify either a through-hardened material or a saturation of the case hardening procedure (e.g., the "plateau" region of the M-50 NiL surface). Thus, the method can be used to examine if the heat treatment process has been properly implemented on a part and is additionally useful in determining how much of the graded layer has been removed during final machining of a component. Finally, any discontinuities noted in the trends of normalized hardness versus load can be attributed to dramatic changes in the subsurface hardness gradient or proximity to the core region with constant hardness.

Acknowledgment

This research was partially supported by the National Science Foundation Award CMMI-0927849 under program officer Dr. Clark V. Cooper and a subcontract from Air Force SBIR grant through UES Inc., Dayton, OH. Authors sincerely acknowledge Mr. Robert Wolfe of Timken Co., Canton, OH, and Dr. Nelson Foster of AFRL, WPAFB, Dayton, OH, and Mr. Hitesh Trivedi of UES Inc., Dayton, OH, for supply of materials for this research.

References

[1] Miyamoto, Y., Kaysser, W. A., and Rabin, B. H., 1999, *Functionally Graded Materials: Design, Processing, and Applications*, 1st ed., Springer, New York.
[2] Suresh, S., and Mortensen, A., 1998, *Fundamentals of Functionally Graded Materials*, Maney Materials Science, Leeds, UK.
[3] Suresh, S., 2001, "Graded Materials for Resistance to Contact Deformation and Damage," Science, **29**(292), pp. 2447–2451.
[4] Ginnakopoulus, A. E., 2002, "Indentation of Plastically Graded Substrates by Sharp Indentors," Int. J. Solid Struct., **39**(9), pp. 2495–2515.
[5] Nakamura, T., Wang, T., and Sampath, S., 2000, "Determination of Properties of Graded Materials by Inverse Analysis and Instrumented Indentation," Acta Mater., **48**(17), pp. 4293–4306.
[6] Gu, Y., Nakamura, T., Prchlik, L., Sampath, S., and Wallace, J., 2003, "Micro-Indentation and Inverse Analysis to Characterize Elastic-Plastic Graded Materials," Mater. Sci. Eng. A, **345**(1–2), pp. 223–233.
[7] Cao, Y. P., Qian, X. Q., Lu, J., and Yao, Z. H., 2005, "An Energy-Based Method to Extract Plastic Properties of Metal Materials From Conical Indentation Tests," J. Mater. Res., **20**(5), pp. 1194–1206.
[8] Cao, Y. P., and Lu, J., 2004, "A New Scheme for Computational Modeling of Conical Indentation in Plastically Graded Materials," J. Mater. Res., **19**(6), pp. 1703–1716.
[9] Choi, I. S., Dao, M., and Suresh, S., 2008, "Mechanics of Indentation of Plastically Graded Materials–I: Analysis," J. Mech. Phys. Solids, **56**(1), pp. 157–171.
[10] Choi, I. S., Detor, A. J., Schwaiger, R., Dao, M., Schuh, C. A., and Suresh, S., 2008, "Mechanics of Indentation of Plastically Graded Materials–II: Expermiments on Nanocrystalline Alloys with Grain Size Gradients," J. Mech. Phys. Solids, **56**(1), pp. 172–183.
[11] Nayebi, A., El Abdi, E., Bartier, O., and Mauvoisin, G., 2002, "New Procedure to Determine Steel Mechanical Parameters From the Spherical Indentation Technique," Mech. Mater. **34**(4), pp. 243–254.
[12] Nayebi, A., El Abdi, E., Bartier, O., and Mauvoisin, G., 2002, "Hardness Profile Analysis of Elasto-Plastic Heat-Treated Steels With a Gradient in Yield Strength," Mater. Sci. Eng. A **333**(1–2), pp. 160–169.
[13] Boyer, H., 1987, *Case Hardening of Steels*, ASTM, Metals Park, OH.
[14] Branch, N. A., Subhash, G., Arakere, N. K., and Klecka, M. A., 2011, "A New Reverse Analysis to Determine the Constitutive Response of Plastically Graded Case Hardened Bearing Steels," Int. J. of Solids Struct., **48**(3–4), pp. 584–591.
[15] Stephens, L. S, Liu, Y., and Meletis, E. I., 2002, "Finite Element Analysis of the Initial Yielding Behavior of a Hard Coating/Substrate System With Functionally Graded Interface Under Indentation and Friction," J. Tribol., **122**(2), pp. 381–387.
[16] Hetzner, D. W., 2004, "Easily Carburizable High-Speed Steel Bearing Alloys," Adv. Mat. Process., **162**(3), pp. 37–39.
[17] Hetzner, D. W., 2006, "Continued Developments in Easily Carburizable High Speed Steel Alloys," J. ASTM Int., **3**(2), pp. 198–206.
[18] Hetzner, D. W. and Van Geertruyden, W., 2008, "Crystallography and Metallography of Carbides in High Alloy Steels," Mater. Charact., **59**(7), pp. 825–841.
[19] ASTM Standard E384, "Standard Test Method for Knoop and Vickers Hardness of Materials," ASTM International, West Conshohocken, PA.
[20] Gao, X. L., Jing, X. N., and Subhash, G., 2006, "Two Expanding Cavity Models for Indentation Deformations of Elastic Strain Hardening Materials," Int. J. of Solids Struct., **43**(7–8), pp. 2193–2208.
[21] Chen, J., and Bull, S. J., 2006, "A Critical Examination of the Relationship Between Plastic Deformation Zone Size and Young's Modulus to Hardness Ratio in Indentation Testing," J. Mater. Res., **21**(10), pp. 2617–2627.
[22] Branch, N. A., Subhash, G., Arakere, N. K., and Klecka, M. A., 2010, "Material Dependent Representative Plastic Strain for the Prediction of Indentation Hardness," Acta Mater., **58**(19), pp. 6487–6494.